Power Flow Analytical Method for Three-phase Active Distribution Networks Based on Multi-Dimensional Holomorphic Embedding Method

Yuge Sun, *Student Member, IEEE*, Tao Ding, *Senior Member, IEEE*, Tianrui Xu, *Student Member, IEEE*, Chenggang Mu, *Student Member, IEEE*, Pierluigi Siano, *Senior Member, IEEE*, João P. S. Catalão, *Fellow, IEEE*

***Abstract*—With the increasing penetration of distributed generations (DGs) in three-phase distribution networks, the traditional radial passive distribution networks are gradually transformed into active distribution networks (ADNs) with DGs, accompanied by a dramatic increase in operational scenarios. To fast analyze the massive scenarios of ADNs, this paper proposes a multi-scenario-based power flow analytical method based on the multi-dimensional holomorphic embedding method. First, DGs are partitioned according to their spatial correlation, and then a power flow analytical method is cast for unbalanced three-phase ADNs. Finally, the method is applied to the ADN power flow analysis for multiple scenarios. Comparisons with other power flow calculation methods validate the high efficiency and computational tractability of the proposed method.**

***Index Terms*—Distributed generation, power flow analytical method, multi-dimensional holomorphic embedding method, unbalanced three-phase active distribution network.**

I. Introduction

Carbon emissions have caused serious climate problems. Replacing traditional fossil fuels with renewable energy resources for power generation is the key to dealing with these problems. Distributed generators (DGs), such as photovoltaic, wind power, etc., ensure a clean and sustainable power supply in distribution networks [1], gradually transforming the traditional radial passive distribution networks into active distribution networks (ADNs) [2].

The high penetration and uncertainty of DGs have amplified the complexity of ADNs and brought considerable challenges to ADN analysis. The access of DGs has dramatically increased the number of operation scenarios of ADNs [3]. Whether planning, operating or reliability analysis of ADNs [4], scholars should comprehensively analyze these massive operation scenarios. Power flow calculation that serves as a basic analysis tool in modern ADN analysis and distribution management system (DMS) [5], should be completed fast and reliably.

The distribution network is different from the transmission network in topology, branch parameters, operation condition, including radial and weakly meshed structure, high R/X ratios, multi-phase and unbalanced operation, a large number of buses and branches, etc. [2]. These characteristics make it necessary to calculate the three-phase unbalanced power flow of the distribution system, not only for the single-phase [6]. Therefore, scholars had proposed power flow calculation methods for three-phase distribution networks according to these characteristics, including the backward-forward sweep (BFS) algorithm [7]-[8], the modified Newton method [9], the direct approach [10], the implicit Z_{Bus} Gauss method [11], the linear power flow (LPF) method [12]-[13], and the current injection method [14], etc.

The above power flow calculation methods generally relied on iterative methods, and the power flow solutions are numerical solutions [15]-[16]. To analyze massive operation scenarios, performing power flow calculations repeatedly is necessary. This is because once the operating conditions change, it is required to recalculate the power flow with a cold start.

Different from the iterative methods, Ref. [17] proposed a recursive method called the holomorphic embedding method (HEM) for transmission network power flow calculation, ensuring that feasible solutions can be found in the convergence region and expressing the power flow solutions as explicit analytical expressions. In [18], a multi-stage HEM scheme was raised to calculate an accurate P-V curve for heavily loaded power systems. Ref. [19] proposed a fast and flexible HEM for solving power flow, which deals with the Q-limit problem and allows any operating state as the initial guess, thus improving the flexibility of HEM. An interval total transfer capability model was established based on multi-dimensional holomorphic embedding method (MDHEM) in [20], considering the renewable energy uncertainties. Moreover, the applications of HEM and its variants were extended to nascent meshed HVDC networks and distribution systems in more-electric vehicles, ships, aircraft, and spacecraft [21]. A HEM-based methodology considering the characteristics of unbalanced radial distribution networks was proposed in [22], where the tap-changer, doubly-fed induction generator, and photovoltaic system are modeled. In [23], two modifications of HEM are presented for solving distribution networks, which exploit the radial and weakly meshed topology and significantly reduce computation time. Starting with the modeling of the three-phase line by Kron reduction and the forming of the system impedance matrix, [24] proposed a modified HEM method for three-phase distribution networks, which used the impedance matrix to eradicate the effect of sparseness in the admittance matrix. Moreover, the

This work was supported in part by National Natural Science Foundation of China (Grant 51977166), in part by Natural Science Foundation of Shaanxi Province (Grant 2022JC-19) and in part by Science and Technological Project of Northwest Branch of State Grid Corporation of China (SGNW0000DKQT2100172). Paper no. TCAS-II-13511-2022. (Corresponding author: Tao Ding, e-mail: tding15@mail.xjtu.edu.cn)

Y. Sun, T. Ding, T. Xu, and C. Mu are with the School of Electrical Engineering, Xi'an Jiaotong University, Xi'an 710049, China.

P. Siano is with the Department of Management & Innovation Systems, University of Salerno, Italy.

J. P. S. Catalão is with the Faculty of Engineering and Institute for Systems and Computer Engineering, University of Porto, 4099-002 Porto, Portugal.

HEM was applied to the power flow calculation of three-phase distribution networks in [25], accommodating DGs and multiple types of loads. In summary, the HEM-based power flow methods can calculate power flow expressions offline in advance, thus the power flow solutions are available by just bringing operation condition values into the expressions.

However, only one variable was embedded in the power flow equations in [25], such that the operation scenarios can only change in the same direction. Thus, the spatial correlation and differences between DGs were not considered. Therefore, we propose an innovative multi-scenario-based power flow analytical method based on MDHEM [26]-[27] for unbalanced three-phase ADNs. The main contributions are threefold:

(i) Considering the spatial correlation and differences of DGs/loads, the DGs/loads connected to the ADNs are divided into multiple regions, and different independent variables are used to control the behaviors of DGs/loads in different regions.

(ii) Based on the modeling of network components, the multi-variable power flow analytical model for unbalanced three-phase ADNs is established by using MDHEM. The multi-variable power flow expressions deduced offline can be applied to fast and easily calculate the multi-scenario power flow. Different from the iterative methods, the proposed method does not need to calculate power flow repeatedly, exhibiting high efficiency in multi-scenario power flow calculation.

(iii) The proposed method can simulate the DGs/loads in different regions change with various directions. Compared with the previous HEM-based power flow methods that can only control the system change uniformly, the proposed method better models the ADNs with frequent state changes and is more flexible and efficient in multi-scenario analysis.

The remainder of the paper is organized as follows. Section II presents the modeling for the basic components in three-phase ADNs. Section III establishes the power flow analytical model based on the MDHEM. Case studies on several standard test cases are presented in Section IV to verify the effectiveness of the proposed method. Section V summarizes the paper.

II. Three-Phase Unbalanced Model for ADNs

To deal with the three-phase unbalanced problems for ADNs, we utilize the phase component method to model the network components in the three-phase unbalanced ADNs with DGs.

A. Modeling for Branch Components

The model of distribution lines is represented as the three-phase π-type equivalent circuit as shown in Fig. 1(a). Bus i and j represent the starting and ending points of line l; V_i^{φ} and I_i^{φ} represent the bus voltage and injection current at bus i on phase φ (φ=a, b, c); $\boldsymbol{Z}$ and $\boldsymbol{Y}_s$ represent the series impedance matrix and the shunt admittance matrix of line l, respectively. The equivalent admittance matrix of line l is expressed in (1). Besides, the three-phase equivalent model of the transformers is exhibited in Fig. 1(b), and the relationship between the bus voltage and the injection current can be expressed as (2).

$$\mathbf{Y}_l = \begin{bmatrix} \mathbf{Z}^{-1} + \mathbf{Y}_s/2 & -\mathbf{Z}^{-1} \\ -\mathbf{Z}^{-1} & \mathbf{Z}^{-1} + \mathbf{Y}_s/2 \end{bmatrix}. \tag{1}$$

$$\begin{bmatrix} \mathbf{I}_p \\ \mathbf{I}_s \end{bmatrix} = \mathbf{Y}_t \begin{bmatrix} \mathbf{V}_p \\ \mathbf{V}_s \end{bmatrix} = \begin{bmatrix} \mathbf{Y}_{pp} & \mathbf{Y}_{ps} \\ \mathbf{Y}_{sp} & \mathbf{Y}_{ss} \end{bmatrix} \begin{bmatrix} \mathbf{V}_p \\ \mathbf{V}_s \end{bmatrix} \tag{2}$$

where $\mathbf{V}_p = [V_p^{\mathrm{A}}, V_p^{\mathrm{B}}, V_p^{\mathrm{C}}]^{\mathrm{T}}$ and $\mathbf{V}_s = [V_s^{\mathrm{a}}, V_s^{\mathrm{b}}, V_s^{\mathrm{c}}]^{\mathrm{T}}$ are the voltages of primary and secondary sides; $\mathbf{I}_p = [I_p^{\mathrm{A}}, I_p^{\mathrm{B}}, I_p^{\mathrm{C}}]^{\mathrm{T}}$ and $\mathbf{I}_s = [I_s^{\mathrm{a}}, I_s^{\mathrm{b}}, I_s^{\mathrm{c}}]^{\mathrm{T}}$ are the injection currents of the primary and secondary sides; $\mathbf{Y}_t$ represents the equivalent admittance matrix.

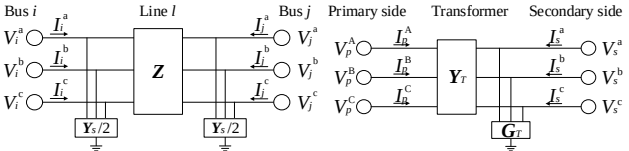

(a) Model of distribution lines (b) Model of distribution transformers

Fig. 1. Three-phase equivalent circuit of transformers.

B. Modeling for Bus Components

Bus components include loads and DGs. The load can be modeled as a Y-connection or a Δ-connection PQ load bus, as shown in Fig. 2. For the Y-connection PQ load bus, the injection current I_i^{φ} can be expressed by the complex power injection S_i^{φ} and the bus voltage V_i^{φ} at bus i on phase φ as (3)

$$I_i^{\varphi} = \left(S_i^{\varphi} / V_i^{\varphi}\right)^* \tag{3}$$

For the Δ-connection PQ load bus, the injection three-phase current $\mathbf{I}_i$ can be expressed as

$$\mathbf{I}_i = \left[I_i^{\mathrm{a}}, I_i^{\mathrm{b}}, I_i^{\mathrm{c}}\right]^T = A_T \left[I_i^{\mathrm{ab}}, I_i^{\mathrm{bc}}, I_i^{\mathrm{ca}}\right]^T, \text{where } A_T = \begin{bmatrix} -1 & 0 & 1 \\ 1 & -1 & 0 \\ 0 & 1 & -1 \end{bmatrix} \tag{4}$$

$$I_i^{\varphi\varphi'} = \left(S_i^{\varphi\varphi'} / V_i^{\varphi\varphi'}\right)^* \tag{5}$$

where I_i^{φ} is the injection current at bus i on phase φ and $I_i^{\varphi\varphi'}$ is the interphase current between phases φ and φ'; $S_i^{\varphi\varphi'}$ is the specified interphase power; $V_i^{\varphi\varphi'}$ is the interphase voltage. Similar to PQ load buses, DGs can also be modeled as constant power components while the injection power is positive.

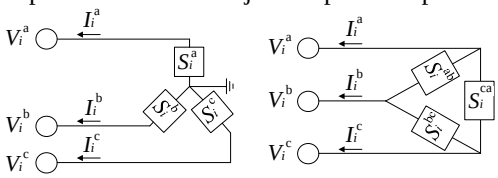

(a) Y-connection PQ load bus (b) Δ-connection PQ load bus

Fig. 2. The three-phase equivalent circuit of loads.

III. Multi-Variable Power Flow Analytical Method for Three-Phase Unbalanced ADNs

Based on the above component models of three-phase ADNs, the explicit power flow expressions for the multi-region three-phase ADNs by using MDHEM can be derived as follows.

A. System Partitioning

HEM is a power flow calculation method based on complex analysis, recursive theory, and analytic continuation. Through the steps of variable embedding, recursive calculation, and Padé Approximants, the original implicit power balance equations (PBEs) can be transformed into explicit PBEs.

Note that a unified variable is embedded into the original PBEs in HEM, thus the final power flow expressions (e.g. bus voltage expressions) are a set of holomorphic functions w.r.t. this unified variable. Physically, this variable can be regarded

as the power-scaling factor which describes the power changes of the whole system. Therefore, embedding a unified variable into PBEs implies that the system operation scenarios can only change in a unified direction. However, a large amount of DGs/loads in a three-phase AND often have a strong spatial correlation in the same region, while their characteristics in different regions are quite different. It is inappropriate to adopt a unified variable to control the power ratio of the whole system.

Therefore, considering bus types and geographical locations, we partition the system into multiple regions, where multiple independent power ratios are adopted to characterize the power variation characteristic of the DGs/loads in different regions.

B. Power Flow Analytical Model

Assume an N-bus three-phase unbalanced ADN with D regions containing a slack bus and (N-1) PQ buses, in which PQ buses are Y-connection or Δ-connection loads and DGs. The PBEs for the ADN are given as

$$\sum_{k=1}^{N}\sum_{m=\mathrm{a}}^{\mathrm{c}} Y_{i\varphi,km}V_k^m = \left(P_i^{\varphi} - \mathrm{j}Q_i^{\varphi}\right)\Big/V_i^{\varphi *}, \quad \forall i \in \text{PQ in Y-connection},\ \varphi = \mathrm{a,b,c}. \tag{6}$$

$$\sum_{k=1}^{N}\sum_{m=\mathrm{a}}^{\mathrm{c}} Y_{ix,km}V_k^m = \left(P_i^{zx} - \mathrm{j}Q_i^{zx}\right)\Big/V_i^{zx*} - \left(P_i^{xy} - \mathrm{j}Q_i^{xy}\right)\Big/V_i^{xy*}, \quad \forall i \in \text{PQ in }\Delta\text{-connection},\ (x,y,z) = \{(\mathrm{a,b,c}),(\mathrm{b,c,a}),(\mathrm{c,a,b})\}. \tag{7}$$

$$V_i^{\varphi} = V_{i,sp}^{\varphi}\angle\theta_{i,sp}^{\varphi}, \forall i \in \text{slack} \tag{8}$$

where $Y_{i\varphi,km}$ is the admittance between bus i at phase φ and bus k at phase m; P_i^{φ}, Q_i^{φ} are the active and reactive powers injected at bus i at phase φ; P_I^{xy}, Q_i^{xy} are the interphase active and reactive powers at bus i between phases x and y; $V_{i,sp}^{\varphi}$, $\theta_{i,sp}^{\varphi}$ are the specified voltage magnitude and phase angle at the slack bus at phase φ; (•)* is the conjugate of a complex number.

Since the ADN is divided into D regions, two complex-valued variables will be embedded into the PBEs for each region to control the change of its active and reactive power, respectively. Therefore, based on MDHEM, the unknown phase voltage V_i^{φ} and interphase voltage $V_i^{\varphi\varphi'}$ will be expressed as holomorphic functions w.r.t. the 2D embedding variables as

$$V_i^{\varphi}\left(s_1, s_2, \cdots, s_{2D}\right) = \sum_{n_{2D}=0}^{\infty}\cdots\sum_{n_2=0}^{\infty}\sum_{n_1=0}^{\infty} v_i^{\varphi}\left[n_1, n_2, \cdots, n_{2D}\right]\cdot s_1^{n_1}s_2^{n_2}\cdots s_{2D}^{n_{2D}} \tag{9}$$

$$V_i^{\varphi\varphi'}\left(s_1, s_2, \cdots, s_{2D}\right) = \sum_{n_{2D}=0}^{\infty}\cdots\sum_{n_2=0}^{\infty}\sum_{n_1=0}^{\infty}\begin{pmatrix} v_i^{\varphi}\left[n_1, n_2, \cdots, n_{2D}\right] \\ -v_i^{\varphi'}\left[n_1, n_2, \cdots, n_{2D}\right]\end{pmatrix}\cdot s_1^{n_1}s_2^{n_2}\cdots s_{2D}^{n_{2D}} \tag{10}$$

where s_1 to s_D and s_{D+1} to s_{2D} represent the variables corresponding to active and reactive powers, respectively; n_e is the power of s_e. Under this setting, solving the unknown coefficients $v_i^{\varphi}[n_1, n_2, \ldots, n_{2D}]$ is the main task of MDHEM.

Firstly, by introducing the holomorphic functions $V_i^{\varphi}(s_1, s_2, \ldots, s_{2D})$ and $V_i^{\varphi\varphi'}(s_1, s_2, \ldots, s_{2D})$ into (6) and (7) respectively, the embedding equations for the initial PBEs can be written as:

$$\sum_{k=1}^{N}\sum_{m=\mathrm{a}}^{\mathrm{c}} Y_{i\varphi,km}V_k^m\left(s_1, s_2, \cdots, s_{2D}\right) = \frac{P_{i0}^{\varphi}\left(1+s_{x(i)}\right) - \mathrm{j}Q_{i0}^{\varphi}\left(1+s_{D+x(i)}\right)}{V_i^{\varphi *}\left(s_1^*, s_2^*, \cdots, s_{2D}^*\right)}, \quad \forall i \in \text{PQ in Y-connection},\ \varphi = \mathrm{a,b,c}. \tag{11}$$

$$\sum_{k=1}^{N}\sum_{m=\mathrm{a}}^{\mathrm{c}} Y_{ix,km}V_k^m\left(s_1, s_2, \cdots, s_{2D}\right) = \frac{P_{i0}^{zx}\left(1+s_{x(i)}\right) - \mathrm{j}Q_{i0}^{zx}\left(1+s_{D+x(i)}\right)}{V_i^{zx*}\left(s_1^*, s_2^*, \cdots, s_{2D}^*\right)} - \frac{P_{i0}^{xy}\left(1+s_{x(i)}\right) - \mathrm{j}Q_{i0}^{xy}\left(1+s_{D+x(i)}\right)}{V_i^{xy*}\left(s_1^*, s_2^*, \cdots, s_{2D}^*\right)}, \tag{12}$$

$\forall i \in$ PQ in Δ-connection, $(x,y,z) = \{(\mathrm{a,b,c}),(\mathrm{b,c,a}),(\mathrm{c,a,b})\}$.

where $x(i)$ represents the region index that bus i belongs to; $s_{x(i)}$ and $s_{D+x(i)}$ represent the power ratio of active and reactive powers at bus i; P_{i0}^{φ}, Q_{i0}^{φ}, P_{i0}^{zx} and Q_{i0}^{zx} are the value of P_i^{φ}, Q_i^{φ}, P_i^{zx} and Q_i^{zx} at the given initial operation condition.

Secondly, replacing the $1/V_i^{\varphi *}(s_1^*, s_2^*, \ldots, s_{2D}^*)$ and $1/V_i^{zx*}(s_1^*, s_2^*, \ldots, s_{2D}^*)$ by $W_i^{\varphi *}(s_1^*, s_2^*, \ldots, s_{2D}^*)$ and $H_i^{zx*}(s_1^*, s_2^*, \ldots, s_{2D}^*)$ gives (13)-(14), where $w_i^{\varphi *}[n_1, n_2, \ldots, n_{2D}]$ and $h_i^{zx*}[n_1, n_2, \ldots, n_{2D}]$ are the coefficients of $s_1^{n_1}\, s_2^{n_2}\ldots\, s_{2D}^{n_{2D}}$, respectively.

$$W_i^{\varphi *}\left(s_1^*, s_2^*, \cdots, s_{2D}^*\right) = 1\Big/V_i^{\varphi *}\left(s_1^*, s_2^*, \cdots, s_{2D}^*\right) = \sum_{n_{2D}=0}^{\infty}\cdots\sum_{n_2=0}^{\infty}\sum_{n_1=0}^{\infty} w_i^{\varphi *}\left[n_1, n_2, \cdots, n_{2D}\right]\cdot s_1^{n_1}s_2^{n_2}\cdots s_{2D}^{n_{2D}} \tag{13}$$

$$H_i^{zx*}\left(s_1^*, s_2^*, \cdots, s_{2D}^*\right) = 1\Big/V_i^{zx*}\left(s_1^*, s_2^*, \cdots, s_{2D}^*\right) = \sum_{n_{2D}=0}^{\infty}\cdots\sum_{n_2=0}^{\infty}\sum_{n_1=0}^{\infty} h_i^{zx*}\left[n_1, n_2, \cdots, n_{2D}\right]\cdot s_1^{n_1}s_2^{n_2}\cdots s_{2D}^{n_{2D}} \tag{14}$$

Furthermore, substituting (13)-(14) into (11)-(12) yields

$$\sum_{k=1}^{N}\sum_{m=\mathrm{a}}^{\mathrm{c}} Y_{i\varphi,km}\left(v_k^m[0,\cdots,0] + v_k^m[1,0,\cdots]s_1 + v_k^m[0,1,\cdots]s_2 + \cdots\right) = \left[P_{i0}^{\varphi}\left(1+s_{x(i)}\right) - \mathrm{j}Q_{i0}^{\varphi}\left(1+s_{D+x(i)}\right)\right]\cdot\left(w_i^{\varphi *}[0,\cdots,0] + w_i^{\varphi *}[1,0,\cdots]s_1 + \cdots\right) \tag{15}$$

$\forall i \in$ PQ in Y-connection, $\varphi = \mathrm{a,b,c}$.

$$\begin{aligned}&\sum_{k=1}^{N}\sum_{m=\mathrm{a}}^{\mathrm{c}} Y_{i\varphi,km}\left(v_k^m[0,\cdots,0] + v_k^m[1,0,\cdots]s_1 + v_k^m[0,1,\cdots]s_2 + \cdots\right) \\ &= \left[P_{i0}^{zx}\left(1+s_{x(i)}\right) - \mathrm{j}Q_{i0}^{zx}\left(1+s_{D+x(i)}\right)\right]\cdot\left(h_i^{zx*}[0,\cdots,0] + h_i^{zx*}[1,0,\cdots]s_1 + \cdots\right) \\ &\quad - \left[P_{i0}^{xy}\left(1+s_{x(i)}\right) - \mathrm{j}Q_{i0}^{xy}\left(1+s_{D+x(i)}\right)\right]\cdot\left(h_i^{xy*}[0,\cdots,0] + h_i^{xy*}[1,0,\cdots]s_1 + \cdots\right),\end{aligned} \tag{16}$$

$\forall i \in$ PQ in Δ-connection, $(x,y,z) = \{(\mathrm{a,b,c}),(\mathrm{b,c,a}),(\mathrm{c,a,b})\}$.

Since the LHS and RHS of (15)-(16) are all power series expressions regarding (s_1, s_2, …, s_{2D}), the recursive equations can be obtained by equating the coefficients of the same term (e.g. $s_1^{n_1}\, s_2^{n_2}\ldots\, s_{2D}^{n_{2D}}$) on both sides of the equations, such that

$$\begin{aligned}&\sum_{k=1}^{N}\sum_{m=\mathrm{a}}^{\mathrm{c}} Y_{i\varphi,km}v_k^m\left[\cdots, n_{x(i)}, \cdots, n_{D+x(i)}, \cdots\right] - \left(P_{i0}^{\varphi} - \mathrm{j}Q_{i0}^{\varphi}\right)w_i^{\varphi *}\left[\cdots, n_{x(i)}, \cdots, n_{D+x(i)}, \cdots\right] \\ &= P_{i0}^{\varphi}w_i^{\varphi *}\left[\cdots, n_{x(i)}-1, \cdots, n_{D+x(i)}, \cdots\right] - \mathrm{j}Q_{i0}^{\varphi}w_i^{\varphi *}\left[\cdots, n_{x(i)}, \cdots, n_{D+x(i)}-1, \cdots\right],\end{aligned} \tag{17}$$

$\forall i \in$ PQ in Y-connection, $\varphi = \mathrm{a,b,c}$.

$$\begin{aligned}&\sum_{k=1}^{N}\sum_{m=\mathrm{a}}^{\mathrm{c}} Y_{i\varphi,km}v_k^m\left[\cdots, n_{x(i)}, n_{D+x(i)}, \cdots\right] - \left(P_{i0}^{zx} - \mathrm{j}Q_{i0}^{zx}\right)h_i^{zx*}\left[\cdots, n_{x(i)}, \cdots, n_{D+x(i)}, \cdots\right] \\ &\quad + \left(P_{i0}^{xy} - \mathrm{j}Q_{i0}^{xy}\right)h_i^{xy*}\left[\cdots, n_{x(i)}, \cdots, n_{D+x(i)}, \cdots\right] \\ &= P_{i0}^{zx}h_i^{zx*}\left[\cdots, n_{x(i)}-1, \cdots, n_{D+x(i)}, \cdots\right] - \mathrm{j}Q_{i0}^{zx}h_i^{zx*}\left[\cdots, n_{x(i)}, \cdots, n_{D+x(i)}-1, \cdots\right] \\ &\quad - P_{i0}^{xy}h_i^{xy*}\left[\cdots, n_{x(i)}-1, \cdots, n_{D+x(i)}, \cdots\right] + \mathrm{j}Q_{i0}^{xy}h_i^{xy*}\left[\cdots, n_{x(i)}, \cdots, n_{D+x(i)}-1, \cdots\right],\end{aligned} \tag{18}$$

$\forall i \in$ PQ in Δ-connection, $(x,y,z) = \{(\mathrm{a,b,c}),(\mathrm{b,c,a}),(\mathrm{c,a,b})\}$.

Equations (17)-(18) give the recursive relations between the coefficients of the expressions $V_i^{\varphi}(s_1, s_2, \ldots, s_{2D})$, $W_i^{\varphi}(s_1, s_2, \ldots, s_{2D})$ and $H_i^{zx}(s_1, s_2, \ldots, s_{2D})$. Observe that the coefficients $v_i^{\varphi}[\bullet]$, $w_i^{\varphi}[\bullet]$ and $h_i^{zx}[\bullet]$ at a required order can always be expressed by the coefficients of their lower orders. Besides, the relationships between $v_i^{\varphi}[\bullet]$ and $w_i^{\varphi}[\bullet]$, $v_i^{zx}[\bullet]$ and $h_i^{zx}[\bullet]$ can be further deduced by (13)-(14). Let the coefficient of the same term on both sides of equations $V_i^{\varphi}(s_1, s_2, \ldots, s_{2D}) = 1/W_i^{\varphi}(s_1, s_2, \ldots, s_{2D})$ and $V_i^{zx*}(s_1, s_2, \ldots, s_{2D}) = 1/H_i^{zx*}(s_1, s_2, \ldots, s_{2D})$ be equal, we have

This article has been accepted for publication in IEEE Transactions on Circuits and Systems--II: Express Briefs. This is the author's version which has not been fully edited and content may change prior to final publication. Citation information: DOI 10.1109/TCSII.2022.3204606

$$\begin{aligned}
&v_{i0}^{\varphi}\cdot w_{i0}^{\varphi}=1, M=0.\\
&v_{i0}^{\varphi}\cdot w_{i}^{\varphi}\left[1,0,\cdots,0\right]+w_{i0}^{\varphi}\cdot v_{i}^{\varphi}\left[1,0,\cdots,0\right]=0, M=1.\\
&v_{i0}^{\varphi}\cdot w_{i}^{\varphi}\left[n_1,n_2,\cdots,n_{2D}\right]+w_{i0}^{\varphi}\cdot v_{i}^{\varphi}\left[n_1,n_2,\cdots,n_{2D}\right]=-\underset{K=1}{\overset{M-1}{Conv}}\left(v_{i}^{\varphi}\cdot w_{i}^{\varphi}\right), M\geq 2.
\end{aligned} \tag{19}$$

$$\begin{aligned}
&\left(v_{i0}^{z}-v_{i0}^{x}\right)\cdot h_{i}^{zx}\left[0,0,\cdots,0\right]=1, M=0.\\
&\left(v_{i0}^{z}-v_{i0}^{x}\right)\cdot h_{i}^{zx}\left[1,0,\cdots,0\right]+h_{i0}^{zx}\cdot\left(v_{i}^{z}\left[1,0,\cdots,0\right]-v_{i}^{x}\left[1,0,\cdots,0\right]\right)=0, M=1.\\
&\left(v_{i0}^{z}-v_{i0}^{x}\right)h_{i}^{zx}\left[n_1,n_2,\cdots,n_{2D}\right]+h_{i0}^{zx}\left(v_{i}^{z}\left[n_1,n_2,\cdots,n_{2D}\right]-v_{i}^{x}\left[n_1,n_2,\cdots,n_{2D}\right]\right)\\
&=-\underset{K=1}{\overset{M-1}{Conv}}\left[\left(v_{i}^{z}-v_{i}^{x}\right)\cdot h_{i}^{zx}\right], M\geq 2.
\end{aligned} \tag{20}$$

where v_{i0}^{φ}, w_{i0}^{φ} and h_{i0}^{zx} are the abbreviations of $v_i^{\varphi}[0,0,\ldots,0]$, $w_i^{\varphi}[0,0,\ldots,0]$ and $h_i^{zx}[0,0,\ldots,0]$, which are the constant terms of their corresponding power series and can be easily obtained at the initial operation condition; M represents the total order of $s_1^{n_1}s_2^{n_2}\ldots s_{2D}^{n_{2D}}$; $Conv(\bullet)$ at $M\geq 2$ can be specifically expressed as:

$$\underset{K=1}{\overset{M-1}{Conv}}\left(v_{i}^{\varphi}\cdot w_{i}^{\varphi}\right)=\sum_{K=1}^{M-1}v_{i}^{\varphi}\left[n_1-k_1,n_2-k_2,\cdots,n_{2D}-k_{2D}\right]\cdot w_{i}^{\varphi}\left[k_1,k_2,\cdots,k_{2D}\right]. \tag{21}$$

$$\underset{K=1}{\overset{M-1}{Conv}}\left[\left(v_{i}^{z}-v_{i}^{x}\right)\cdot h_{i}^{zx}\right]=\sum_{K=1}^{M-1}\begin{pmatrix}v_{i}^{z}\left[n_1-k_1,\cdots,n_{2D}-k_{2D}\right]\\-v_{i}^{x}\left[n_1-k_1,\cdots,n_{2D}-k_{2D}\right]\end{pmatrix}\cdot h_{i}^{zx}\left[k_1,\cdots,k_{2D}\right]. \tag{22}$$

$$K=k_1+k_2+\cdots+k_{2D},\quad 0\leq k_s\leq n_s, s=1\sim 2D \tag{23}$$

Overall, (17)-(20) jointly constitute the recursive equations of the power flow analytical model. The coefficients required at any order (LHS of equations) are linearly expressed by the coefficients at their lower orders. Once the germ solution is determined, all coefficients of the power flow expressions can be gradually obtained from the lower order to the higher order.

However, the power flow expressions with finite terms are only truncated series. To obtain more accurate approximants to the holomorphic functions than truncated series, the rational approximants are used to gain the final power flow expressions (24). The unknown $\alpha_i^{\varphi}[\mathbf{p}]$ and $\beta_i^{\varphi}[\mathbf{q}]$ are available by equating the coefficients of the same terms on both sides of (24).

$$\begin{aligned}
&V_i^{\varphi}(\mathbf{s})\doteq A_{\mathbf{X}/\mathbf{Y}}^{\varphi}(\mathbf{s})=\sum_{\mathbf{p}\in I_{\mathbf{X}}}\alpha_i^{\varphi}[\mathbf{p}]\cdot\mathbf{s}^{\mathbf{p}}\Big/\sum_{\mathbf{q}\in I_{\mathbf{Y}}}\beta_i^{\varphi}[\mathbf{q}]\cdot\mathbf{s}^{\mathbf{q}},\\
&where\ \ I_{\mathbf{X}}=\{\mathbf{p}\,|\,\mathbf{0}\leq\mathbf{p}\leq\mathbf{X}\}, I_{\mathbf{Y}}=\{\mathbf{q}\,|\,\mathbf{0}\leq\mathbf{q}\leq\mathbf{Y}\}.\\
&\mathbf{s}=(s_1,s_2,\cdots,s_{2D}),\mathbf{p}=(p_1,p_2,\cdots,p_{2D}),\mathbf{q}=(q_1,q_2,\cdots,q_{2D}),\\
&\mathbf{s}^{\mathbf{p}}=s_1^{p_1}s_2^{p_2}\cdots s_{2D}^{p_{2D}},\mathbf{s}^{\mathbf{q}}=s_1^{q_1}s_2^{q_2}\cdots s_{2D}^{q_{2D}}.
\end{aligned} \tag{24}$$

IV. Case Study

A. Test on the Modified IEEE 123-bus Distribution Network

The proposed method is demonstrated on the modified IEEE 123-bus distribution network. The topology and configuration of DGs are shown in Fig. 3. Numerical results are obtained by using MATLAB on a personal computer with Intel® Core™ i5-11300H CPU @3.1GHz. The system is divided into 6 regions according to the spatial characteristics of DGs/loads, and the power ratios s_1-s_6 are embedded to specify the regional power changes independently. Based on the proposed method, the 6-variable power flow expressions with 1716 terms and their fractional rational approximation expressions with the maximum power of 6 are obtained. Comparisons of the proposed method with BFS are shown in Table I. The proposed method is performed with high computational accuracy.

The total calculation time of the proposed method can be divided into the time for physical germ solution calculation (Step 1), recursive calculation (Step 2), rational approximants (Step 3), and power flow calculation at the current operation scenario (Step 4). In a single scenario, the total time of the proposed method is longer than that of the BFS. However, the proposed method can solve the power flow expressions offline in advance by closed forms (i.e., Step1-Step3). Once the network topology is given, these three steps are fixed and calculated only once. Hence, the power flow calculation time of a single scenario is only the time to take the values of DGs/loads into the expressions (i.e., 0.0006s in Step 4 for the online application), which is shorter than that of BFS.

Furthermore, the power flow calculations for massive operation scenarios are analyzed. The variation characteristics of variables s_1-s_6 are shown in Fig. 4(a). The power flow results are shown in Fig. 4(b). For 1×10^5 operation scenarios, the online calculation time of the proposed method is 2.52s, while that of the BFS is 340.83s, fully showing that the proposed method has a greater efficiency for multi-scenario power flow analysis.

B. Performance Analysis for Multi-Scenario Power Flow

Table II compares the performance of the proposed method and other 6 power flow calculation methods for 4 unbalanced three-phase ADNs, including the modified 37-bus, 123-bus, 906-bus, and 1811-bus systems, so as to compare the accuracy and calculation time of massive operation scenarios.

TABLE I. Comparisons of Two Methods for Calculation Performance

Accuracy (p.u.)				**Time (s)**				
Maximum error				*The proposed method*				*BFS*
V	*θ*	*P*	*Q*	Offline	*Step1*	*Step2*	*Step3*	
5e^{-7}	1e^{-6}	5e^{-10}	4e^{-10}		0.01	69.37	151.82	0.0035
				Online	*Step4*: 0.0006			

TABLE II Comparison of six methods for the solution and computation performance on four ADMs

ADN	Number of Regions	Power Ratio	Scenarios	Time for PM (s)	BFS [7]			MF_BFS [8]			DA [10]			LPF [13]			CIM [14]			HEM [24]		
					Error (p.u.)		Time (s)	Error (p.u.)		Time (s)	Error (p.u.)		Time (s)	Error (p.u.)		Time (s)	Error (p.u.)		Time (s)	Error (p.u.)		Time (s)
					V	*θ*	/	*V*	*θ*	/	*V*	*θ*	/	*V*	*θ*	/	*V*	*θ*	/	*V*	*θ*	/
37	4	[1,3]	1e^4	**0.06**	8e^{-7}	2e^{-5}	6.84	8e^{-7}	2e^{-5}	3.92	8e^{-7}	2e^{-5}	0.51	2e^{-4}	2e^{-3}	31.43	8e^{-7}	2e^{-5}	35.59	8e^{-7}	2e^{-5}	221.5
			1e^5	**0.53**	8e^{-7}	2e^{-5}	64.77	8e^{-7}	2e^{-5}	40.19	8e^{-7}	2e^{-5}	5.04	2e^{-4}	2e^{-3}	328.3	8e^{-7}	2e^{-5}	338.2	8e^{-7}	2e^{-5}	2109
123	6	[1,3]	1e^4	**0.25**	2e^{-6}	2e^{-4}	33.31	2e^{-6}	2e^{-4}	23.46	2e^{-6}	2e^{-4}	5.43	1e^{-4}	6e^{-3}	114.8	2e^{-6}	2e^{-4}	78.27	2e^{-6}	2e^{-4}	644.1
			1e^5	**2.66**	2e^{-6}	2e^{-4}	339.5	2e^{-6}	2e^{-4}	211.5	2e^{-6}	2e^{-4}	51.75	1e^{-4}	6e^{-3}	1136	2e^{-6}	2e^{-4}	790.7	2e^{-6}	2e^{-4}	6437
906	6	[1,3]	1e^4	**1.14**	3e^{-6}	2e^{-4}	243.1	3e^{-6}	2e^{-4}	173.7	3e^{-6}	2e^{-4}	94.97	2e^{-4}	1e^{-2}	561	3e^{-6}	2e^{-4}	347.7	3e^{-6}	2e^{-4}	1871
			1e^5	**11.66**	3e^{-6}	2e^{-4}	2349	3e^{-6}	2e^{-4}	1767	3e^{-6}	2e^{-4}	987.8	2e^{-4}	1e^{-2}	5527	3e^{-6}	2e^{-4}	3696	3e^{-6}	2e^{-4}	×
1811	6	[1,3]	1e^4	**3.47**	1e^{-5}	9e^{-4}	506.4	1e^{-5}	9e^{-4}	354.2	1e^{-5}	9e^{-4}	117.9	7e^{-4}	9e^{-2}	638.1	1e^{-5}	9e^{-4}	444.5	1e^{-5}	9e^{-4}	2047
			1e^5	**35.86**	1e^{-5}	9e^{-4}	5121	1e^{-5}	9e^{-4}	3632	1e^{-5}	9e^{-4}	1115	7e^{-4}	9e^{-2}	6390	1e^{-5}	9e^{-4}	4348	1e^{-5}	9e^{-4}	×

Note: 'PM'-Proposed Method, 'BFS'-Backward-Forward Sweep, 'MF_BFS'-Matricial Formulation of Backward-Forward Sweep, 'DA'-Direct Approach, 'LPF'-Linearize Power Flow, 'CIM'-Current Injection Method. 'Error' refers to the average error between PM and the other method. '×' means too long to measure.

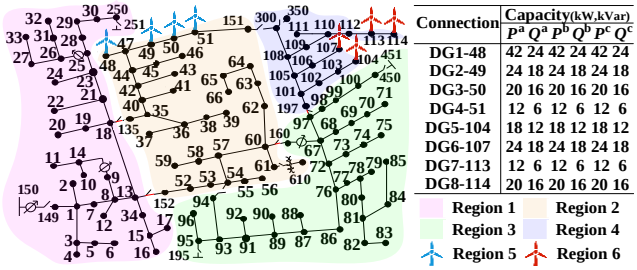

Connection	Capacity(kW,kVar)					
	P^a	Q^a	P^b	Q^b	P^c	Q^c
DG1-48	42	24	42	24	42	24
DG2-49	24	18	24	18	24	18
DG3-50	20	16	20	16	20	16
DG4-51	12	6	12	6	12	6
DG5-104	18	12	18	12	18	12
DG6-107	24	18	24	18	24	18
DG7-113	12	6	12	6	12	6
DG8-114	20	16	20	16	20	16

Fig. 3. The IEEE 123-bus distribution network

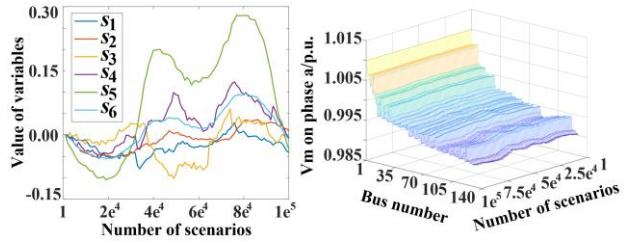

(a) Characteristics of variables (b) Power flow results

Fig. 4. Multi-scenario power flow calculation.

We can conclude that the proposed method has the same high calculation accuracy as other methods except for LPF in the power flow calculation. The calculation time of the proposed method is depended on the system scales and the number of scenarios, and the calculation efficiency is much higher than that of any other method. Note that even the HEM method cannot describe the massive scenarios generated by the independent change of DGs/loads with different ratios, thus it also requires to evaluate the power flow expressions repeatedly, resulting in the most time-consuming. In particular, in the large-scale 1811-bus ADN, the time spent by the proposed method (35.86s) to calculate $1e^5$ scenarios is still much lower than that of other methods (≥1115s), which indicates that the proposed method can be applied to multi-scenario-based power flow calculation of large-scale systems.

V. Conclusion

In this paper, we proposed a multi-scenario-based power flow analytical method for unbalanced three-phase ADNs based on MDHEM. It can be applied to both radial and weakly looped distribution networks. The proposed method can calculate the multi-variable power flow expressions, with different independent variables as the power-scaling factor of each region. It overcomes the disadvantage that the HEM-based method is difficult to describe the massive scenarios of renewable energy bases with only one variable. Compared with other iterative methods, the proposed method is proven to have high accuracy and efficiency in massive operation scenario analysis. It is expected to provide decision support in planning, probabilistic power flow, and reliability analysis of ADNs.

References

[1] G. Liu, C. Yuan, X. Chen, et al, "A High-Performance Energy Management System Based on Evolving Graph," *IEEE Trans. Circuits Syst. II Express Briefs*, vol. 67, no. 2, pp. 350-354, Feb. 2020.

[2] C. S. Cheng and D. Shirmohammadi, "A three-phase power flow method for real-time distribution system analysis," *IEEE Trans. Power Syst.*, vol. 10, no. 2, pp. 671-679, May 1995.

[3] P. Khetrapal, "Distributed Generation: A Critical Review of Technologies, Grid Integration Issues, Growth Drivers and Potential Benefits," *Int. J. Renew. Energy Dev.-IJRED*, vol. 9, no. 2, pp. 189-205, Jul. 2020.

[4] T. Ding, et al, "Multi-Period Active Distribution Network Planning Using Multi-Stage Stochastic Programming and Nested Decomposition by SDDIP," *IEEE Trans. Power Syst.*, vol. 36, no. 3, pp. 2281-2292, 2021.

[5] O. D. Montoya, et al, "Triangular Matrix Formulation for Power Flow Analysis in Radial DC Resistive Grids With CPLs," *IEEE Trans. Circuits Syst. II Express Briefs*, vol. 67, no. 6, pp. 1094-1098, June 2020.

[6] U. Sur, et al, "A Sufficient Condition for Multiple Load Flow Solutions Existence in Three Phase Unbalanced Active Distribution Networks," *IEEE Trans. Circuits Syst. II Express Briefs*, vol. 65, pp. 784-788, 2018.

[7] D. Thukaram, H. M. W. Banda, and J. Jerome, "A robust three phase power flow algorithm for radial distribution systems," *Electr. Power Syst. Res.*, vol. 50, no. 3, pp. 227-236, Jun. 1999.

[8] M. G. Oscar, G. G. Walter, A. G. Diego, "On the Matricial Formulation of Iterative Sweep Power Flow for Radial and Meshed Distribution Networks with Guarantee of Convergence," *Appl. Sci.*. vol. 10. pp. 1-21.

[9] F. Zhang and C. S. Cheng, "A modified Newton method for radial distribution system power flow analysis," *IEEE Trans. Power Syst.*, vol. 12, no. 1, pp. 389-397, Feb. 1997.

[10] J.-H. Teng, "A direct approach for distribution system load flow solutions," *IEEE Trans. Power Delivery*, vol. 18, no. 3, pp. 882–887, 2003.

[11] T. Chen, M. Chen, K. Hwang, P. Kotas and E. A. Chebli, "Distribution system power flow analysis-a rigid approach," *IEEE Trans. Power Delivery*, vol. 6, no. 3, pp. 1146-1152, July 1991.

[12] O. D. Montoya, "On Linear Analysis of the Power Flow Equations for DC and AC Grids With CPLs," *IEEE Trans. Circuits Syst. II Express Briefs*, vol. 66, no. 12, pp. 2032-2036, Dec. 2019.

[13] H. Ahmadi, J. R. Martı´ and A. von Meier, "A Linear Power Flow Formulation for Three-Phase Distribution Systems," *IEEE Trans. Power Syst.*, vol. 31, no. 6, pp. 5012-5021, Nov. 2016.

[14] P. A. N. Garcia, J. L. R. Pereira, S. Carneiro, V. M. da Costa and N. Martins, "Three-phase power flow calculations using the current injection method," *IEEE Trans. Power Sys.*, vol. 15, no. 2, pp. 508-514, May 2000.

[15] F. Bizzarri, D. d. Giudice, D. Linaro and A. Brambilla, "Numerical Approach to Compute the Power Flow Solution of Hybrid Generation, Transmission and Distribution Systems," *IEEE Trans. Circuits Syst. II Express Briefs*, vol. 67, no. 5, pp. 936-940, May 2020.

[16] H. D. Chiang and M. E. Baran, "On the existence and uniqueness of load flow solution for radial distribution power networks," *IEEE Trans. Circuits Syst.*, vol. 37, no. 3, pp. 410-416, March 1990.

[17] A. Trias, "The Holomorphic Embedding Load Flow method," *in Proc. IEEE Power Energy Society General Meeting*, CA, 2012, pp. 1-8.

[18] B. Wang, C. Liu and K. Sun, "Multi-Stage Holomorphic Embedding Method for Calculating the Power-Voltage Curve," *IEEE Trans Power Syst.*, vol. 33, no. 1, pp. 1127-1129, Jan. 2018.

[19] H. -D. Chiang, T. Wang and H. Sheng, "A Novel Fast and Flexible Holomorphic Embedding Power Flow Method," *IEEE Trans. Power Syst.*, vol. 33, no. 3, pp. 2551-2562, May 2018.

[20] Y. Sun, T. Ding, M. Qu, et al, "Interval Total Transfer Capability for Mesh HVDC Systems Based on Sum of Squares and Multi-Dimensional Holomorphic Embedding Method," *IEEE Trans. Power Syst.*, early access.

[21] A. Trias and J. L. Marín, "The Holomorphic Embedding Load flow Method for DC Power Systems and Nonlinear DC Circuits," *IEEE Trans Circuits Syst I Regul Pap.*, vol. 63, no. 2, pp. 322-333, Feb. 2016.

[22] D. Keihan Asl, et al, "Holomorphic embedding load flow for unbalanced radial distribution networks with DFIG and tap-changer modelling," *IET Gener. Transm. Distrib.*, vol. 13, no. 19, pp. 4263-4273, 2019.

[23] M. Heidarifar, et al, "Efficient Load Flow Techniques Based on Holomorphic Embedding for Distribution Networks," *in 2019 IEEE Power & Energy Society General Meeting*, 2019, pp. 1-5.

[24] U. Sur, A. Biswas, J. Bera and G. Sarkar, "A Modified Holomorphic Embedding Load Flow Method for Active Power Distribution Networks," *in 2019 IEEE Region 10 Symposium (TENSYMP)*, 2019, pp. 733-737.

[25] L. Sun, et al, "Holomorphic Embedding Load Flow Modeling of the Three-phase Active Distribution Network," *in 2018 International Conference on Power System Technology*, 2018, pp. 488-495.

[26] C. Liu, B. Wang, X. Xu, K. Sun, D. Shi and C. L. Bak, "A Multi-Dimensional Holomorphic Embedding Method to Solve AC Power Flows," *IEEE Access*, vol. 5, pp. 25270-25285, 2017.

[27] Y. Sun, et al, "Tight Semidefinite Relaxation for Interval Power Flow Model Based on Multi-Dimensional Holomorphic Embedding Method," *IEEE Trans. Power Syst.*, vol. 36, no. 3, pp. 2138-2148, 2021.